

Global Anisotropy Versus Small-Scale Fluctuations in Neutrino Flux in Core-Collapse Supernova Explosions

Hideki Madokoro

madokoro@postman.riken.go.jp

Tetsuya Shimizu

tss@postman.riken.go.jp

and

Yuko Motizuki

motizuki@riken.go.jp

RIKEN, Hirosawa 2-1, Wako 351-0198, Japan

ABSTRACT

Effects of small-scale fluctuations in the neutrino radiation on core-collapse supernova explosions are examined. Through a parameter study with a fixed radiation field of neutrinos, we find substantial differences between the results of globally anisotropic neutrino radiation and those with fluctuations. As the number of modes of fluctuations increases, the shock positions, entropy distributions, and explosion energies approach those of spherical explosion. We conclude that global anisotropy of the neutrino radiation is the most effective mechanism of increasing the explosion energy when the total neutrino luminosity is given. This supports the previous statement on the explosion mechanism by Shimizu and coworkers.

Subject headings: hydrodynamics—shock waves—stars:neutron—supernovae:general

1. INTRODUCTION

For many years since the first work of Colgate & White (1966), numerical simulations of core-collapse supernova explosions have been exciting topics. Until the beginning of the 1990s, almost all the simulations included the assumption of spherical symmetry (e.g.,

Wilson 1985). Such one-dimensional simulations, however, were unable to explain the observed explosion energy and often failed to produce explosions (see, e.g., Liebendoerfer et al. (2001)). Inclusion of convective motion via the mixing length theory cures this problem to some extent (Wilson & Mayle 1993; Bruenn, Mezzacappa, & Dineva 1995). However, spherical simulations based only on the Rayleigh-Taylor instability require considerably large initial fluctuations in density to explain the large-scale matter mixing. In addition, aspherical explosion is also supported by the observation of SN1987A, where asymmetric ejecta are clearly observed (e.g., Wang et al. 2002). These lead us to multidimensional simulations of supernova explosions.

At this time, the two- and three-dimensional simulations have been performed by several groups (Miller, Wilson, & Mayle 1993; Herant et al. 1994; Burrows, Hayes, & Fryxell 1995; Janka & Müller 1996; Mezzacappa et al. 1998; Fryer & Heger 2000; Shimizu et al. 2001; Fryer & Wallen 2002; Kifonidis et al. 2003). In many multidimensional simulations, special attention is paid to the role of convection either near the surface of a nascent neutron star or in neutrino-heated regions above the neutrinosphere. It has been shown that large-scale mixing, caused by convection and convective overturn around the neutrino-heated region, increases the explosion energy and can trigger a successful explosion (Herant et al. 1994; Keil, Janka, & Müller 1996; Janka & Müller 1996).

Because supernova progenitors such as OB stars are generally observed to be fast rotators ($\sim 200 \text{ km s}^{-1}$ at the surface, $P \sim 1$ day; see, e.g., Tassoul 1978; Fukuda 1982), the resulting proto-neutron star can have a large amount of angular momentum after the gravitational collapse. Centrifugal force then deforms the rotating core into an oblate form. This will cause asymmetric neutrino radiation, in which the flux along the pole is enhanced over that on the equatorial plane. Janka & Mönchmeyer (1989) first discussed the possibility of aspherical neutrino emission from a rapidly rotating inner core. They intended to evaluate the total neutrino energy outputs using the neutrino data of SN 1987A detected with the Kamiokande and Irvine-Michigan-Brookhaven experiments. It was argued in their paper that a neutrino flux along the pole might be up to a factor of 3 greater than that on the equatorial plane.

Inspired by this work, Shimizu and coworkers (Shimizu, Yamada, & Sato 1994; Shimizu et al. 2001) proposed that the anisotropic neutrino radiation should play a critical role in the explosion mechanism itself, and carefully investigated the effects of anisotropic neutrino radiation on the explosion energy. They found that only a few percent enhancement in the neutrino emission along the pole is sufficient to increase the explosion energy by a large factor, and that this effect saturates around a certain degree of anisotropy. It should be noted here that the assumed rotational velocity of the inner core is very different between Janka &

Mönchmeyer (1989) and Shimizu et al. (1994, 2001). Shimizu et al. (2001) concluded that the increase in the explosion energy due to anisotropic neutrino radiation occurs because cooling due to neutrino reemission is suppressed in anisotropic models. This is due to earlier shock revival and hence more efficient decrease of the matter temperature than those in spherical models. On the other hand, the neutrino heating itself is almost unchanged by the effect of anisotropic neutrino radiation. The neutrino heating dominates the cooling as a result, which increases the explosion energy, and leads to a successful explosion.

In Shimizu et al. (2001), the geometric effects of neutrino radiation have been rigorously treated outside the neutrinosphere for the first time, although its flux on the neutrinosphere was assumed. Only a global form of anisotropy was assumed there; the maximum peak in the neutrino flux distribution was located at the pole, and the minimum at the equatorial plane. However, Burrows et al. (1995) have suggested that the neutrino flux can fluctuate with angle and time. Such fluctuations are due to gravitational oscillation on the surface of the proto–neutron star and have a completely different origin from that of globally anisotropic neutrino radiation. Thus, it is interesting to investigate how the small-scale fluctuations affect the explosion mechanism and compare the results with those of the global anisotropy.

In this paper, we therefore introduce fluctuations in the neutrino flux in our numerical code by modifying the angular distribution of the neutrino flux. We aim to study the effects of these small-scale fluctuations on the shock position, the explosion energy, and the asymmetric explosion. Our numerical simulation is described in § 2, and the results are presented and discussed in § 3. Our conclusion is given in § 4.

2. NUMERICAL SIMULATION

Our simulation is performed by solving two-dimensional hydrodynamic equations in spherical coordinates. A generalized Roe’s method is employed to solve the hydrodynamic equations with general equations of state (EOSs). The details of our numerical technique, together with the EOS and the initial condition used, are described in the previous article (Shimizu et al. 2001). In our study, we have improved the numerical code of Shimizu et al. (2001); the cells in the θ -direction were shifted by half of the cell size (Shimizu 1995) in order to avoid a numerical error near the pole, although the error was not serious for the investigation of the explosion energy. The computational region is divided into 500 (r -direction) \times 62 (θ -direction) numerical cells.

In the present paper, the local neutrino flux is assumed to be

$$l_\nu(r, \theta) = \frac{7}{16} \sigma T_\nu^4 c_1 (1 + c_2 \cos^2(n_\theta \theta)) \frac{1}{r^2}, \quad (1)$$

where σ is the Boltzmann constant, and T_ν is the temperature on the neutrinosphere. In equation (1), the parameter c_2 represents the magnitude of anisotropy, and n_θ the number of waves in the θ -direction. The case of $n_\theta = 1$ corresponds to the global anisotropy, namely, no fluctuation. We see in equation (1) that the neutrino fluxes in the x (equatorial) and z (polar) directions become $l_x \equiv l_\nu(r, \theta = 90^\circ) \propto c_1$ and $l_z \equiv l_\nu(r, \theta = 0^\circ) \propto c_1(1 + c_2)$, respectively. The degree of anisotropy l_z/l_x is then represented as

$$\frac{l_z}{l_x} = 1 + c_2. \quad (2)$$

Note that equation (2) is different from that defined by Shimizu et al. (2001), $(l_z/l_x)_{\text{Shimizu}}$; for $n_\theta = 1$ and sufficiently small c_2 , we can relate them as $c_2 \sim [(l_z/l_x)_{\text{Shimizu}}^2 - 1]/2$.

The value of c_1 is calculated from given c_2 and n_θ so as to adjust the total neutrino flux to that in the spherical model. The total neutrino luminosity is obtained by integrating equation (1) over the whole solid angle,

$$L_\nu = \int r^2 l_\nu(r, \theta) d\Omega = \frac{7}{16} \sigma T_\nu^4 4\pi c_1 \left(1 + c_2 \frac{2n_\theta^2 - 1}{4n_\theta^2 - 1} \right), \quad (3)$$

which is equated to that of spherical explosion with the same T_ν ,

$$L_\nu^{\text{sp}} = \frac{7}{16} \sigma T_\nu^4 4\pi R_{\text{NS}}^2. \quad (4)$$

In the above, R_{NS} is the radius of a proto-neutron star and fixed to be 50 km. By comparing equations (3) with (4), we obtain

$$c_1 = \frac{R_{\text{NS}}^2}{1 + c_2 (2n_\theta^2 - 1)/(4n_\theta^2 - 1)}. \quad (5)$$

It should be noted here that the magnitude of fluctuations in the neutrino flux distribution for an observer far from the neutrinosphere (represented by c_2) and that on the neutrino-emitting surface (here we denote it as a) are different: the local neutrino flux is seen as equation (1) when we observe fluctuations on the surface of neutrino emission far from the neutrinosphere. It is preferable that we compare the results for the same value of a , since a is more directly related to explosion dynamics. The value of c_2 should, therefore, be calculated from a given a , depending on n_θ . Although it is difficult to calculate the exact relationship between c_2 and a , we can estimate it as follows. First, we assume that the strength of the

neutrino flux on the neutrinosphere is represented by a profile of step functions:

for $n_\theta = 1$

$$f(\theta) \propto \begin{cases} 1 + a & (1 \geq \cos \theta > 1/2) \\ 1 & (1/2 > \cos \theta \geq 0), \end{cases}$$

for $n_\theta = 3$

$$f(\theta) \propto \begin{cases} 1 + a & (1 \geq \cos \theta > 3/4, 1/2 > \cos \theta > 1/4) \\ 1 & (3/4 > \cos \theta > 1/2, 1/4 > \cos \theta \geq 0), \end{cases}$$

for $n_\theta = 5$

$$f(\theta) \propto \begin{cases} 1 + a & (1 \geq \cos \theta > 5/6, 2/3 > \cos \theta > 1/2, 1/3 > \cos \theta > 1/6) \\ 1 & (5/6 > \cos \theta > 2/3, 1/2 > \cos \theta > 1/3, 1/6 > \cos \theta \geq 0). \end{cases}$$

(6)

We continue similarly for larger values of n_θ . The parameter a in equation (6) represents the magnitude of fluctuations in the neutrino flux on the neutrino emitting surface; the bright regions ($f \sim 1 + a$) correspond to those where rising convective motion occurs, while the dark regions ($f \sim 1$) correspond to those of sinking convection. We have assumed that the areas of bright and dark regions are the same. Note that the neutrino flux function is always bright ($f \sim 1 + a$) when $\theta = 0$ (along the pole) and dark ($f \sim 1$) in the case of $\theta = \pi/2$ (on the equatorial plane), and that the fluctuations are essentially added to the global anisotropic model ($n_\theta = 1$).

The neutrino flux observed far from the neutrinosphere is obtained by averaging all contributions from the flux on the surface of the neutrinosphere, $l(\Theta) = \int d\phi \int d\theta f(\theta) \sin \theta \cos(\theta - \Theta)$. Here Θ is the inclination angle between the line of sight of an observer and the polar axis of the proto-neutron star. This means that fully geometric effects from an anisotropically radiating surface are included in neutrino radiation field. For example, there is a contribution from fluxes along the pole axis to those on the equatorial plane, which will tend to reduce an efficiency of anisotropy. The ratio of the local neutrino flux along the polar axis (l_z) to that on the equatorial plane (l_x) for an observer far from the neutrinosphere is described as

$$\begin{aligned} \frac{l_z}{l_x} &= \frac{\int_0^{2\pi} d\phi \int_0^{\pi/2} f(\theta) \sin \theta \cos \theta d\theta}{\int_0^\pi d\phi \int_0^\pi f(\theta) \sin \theta \cos(\theta - \pi/2) d\theta} \\ &= \begin{cases} \frac{1 + 0.750a}{1 + 0.391a} & \text{for } n_\theta = 1, \\ \frac{1 + 0.625a}{1 + 0.438a} & \text{for } n_\theta = 3, \\ \frac{1 + 0.583a}{1 + 0.457a} & \text{for } n_\theta = 5, \dots \end{cases} \end{aligned} \quad (7)$$

By comparing equation (7) with equation (2), we finally obtain the value of c_2 for each value of n_θ .

In the following, we examine two model series: $a = 0.31$ (model series A) and $a = 0.71$ (model series B). These values of a are chosen in such a way that the value of l_z/l_x for the global model ($n_\theta = 1$) becomes 1.10 and 1.20, respectively. The values of c_2 for each fluctuation model ($n_\theta = 3, 5$) are accordingly calculated. These are summarized in Table 1. The neutrino temperature on the neutrino-emitting surface T_ν is assumed to be 4.65 and 4.70 MeV. Note that the value of $1+a$, 1.71, for the model series B roughly corresponds to the variation in the neutrino flux obtained by Burrows et al. (1995), which is at a factor of 1.6.

3. RESULTS AND DISCUSSION

Figures 1 and 2 show the color-scale maps of the dimensionless entropy (Shimizu et al. 2001) distribution with the velocity fields for the model of global anisotropy ($n_\theta = 1$; models A1-T470 and B1-T470). At $t = 82$ ms after the shock stall, the shock front reaches $r \sim 430$ km on the equatorial plane and $r \sim 530$ km at the pole for the model A1-T470. The shock front is prolate, since the neutrino heating along the pole is more intensive than that on the equatorial plane, resulting in a jetlike explosion. At a later stage ($t = 244$ ms), the shock wave is around a few thousand kilometers with large distortion. The entropy distribution of the model B1-T470 has a similar profile except that the shock front is more extended.

In Figures 3 and 4, the results for models with fluctuations (models A3-T470, A5-T470, B3-T470, and B5-T470) are depicted. When $n_\theta = 3$, we find that the degree of asymmetry is smaller than that of the global anisotropy. In particular, the shock position for these models is less extended than the globally anisotropic one. This trend becomes more obvious for the model of $c_2 = +0.035$ and $n_\theta = 5$ (model A5-T470), where the shock front is almost spherical and its radius is only about 1300 km. In the case of the model B5-T470, the shock front is distorted because of a strong hydrodynamic flow along the pole, although this does not affect the explosion energy (see discussion on the energy later in this section).

The profile of the explosion energy is found to be closer to that of spherical explosion as the mode number of fluctuations increases. Figure 5 shows the evolution of the explosion energy, as well as the thermal, kinetic, and gravitational energies for the models of $T_\nu = 4.70$ MeV. The difference between the globally anisotropic model and the models with fluctuations is prominent: the energy gain for the case of $n_\theta = 1$ is the highest among others at all stages of the explosion. It is also seen that the explosion energy decreases as the mode number of

fluctuations in the neutrino flux increases and finally approaches that of spherical explosion. For series B, we have obtained similar results. We observe that asymmetry in explosive motion is more enhanced than that for each model of series A.

In Figure 5, we compare the results of the explosion energy for the two model series. No significant difference is found between the two, although the result of the model A1-T470 becomes larger than that of the model B1-T470 at the later stages of the explosion. It has been shown (Shimizu et al. 2001) that the explosion energy increases as the degree of anisotropy becomes larger for not so large a degree of anisotropy, and finally saturates at $(l_z/l_x)_{\text{Shimizu}} \sim 1.2$. Our new result shows that the final explosion energy of the more anisotropic model B1-T470 is smaller than that of the model A1-T470 (see Fig. 5). The difference may be attributed to the fact that the assumed forms of the local neutrino flux are different (compare eq. [1] here with eq. [5] in Shimizu et al. 2001). In the present paper, we have assumed the form of the neutrino fluxes that has more sharply concentrated flux on the pole. Therefore, the neutrino heating and rising convection are focused on the pole, and those in the equatorial direction are extremely reduced. The shock wave of the model B1-T470 appears to be too weak on the equatorial plane at $t \gtrsim 300\text{ms}$, which causes a energy loss (Shimizu et al. 2001). Such features are clearly seen in the entropy distribution of the model B1-T470.

The effectiveness of global anisotropy becomes more pronounced as T_ν is decreased. Figure 6 shows the same energy evolution as Figure 5, except for $T_\nu = 4.65$ MeV. The difference between the model with global anisotropy and those with fluctuations is extremely remarkable. The globally anisotropic models succeed, while all the other fluctuated and spherical models fail to explode except for the model B3-T465. Note that difference in the neutrino temperature is only 1%, which indicates a sensitivity of the supernova problem on the neutrino luminosity and energy. Note also that an increase of the explosion energies of the models with fluctuations at $t \sim 500$ ms is physically meaningless, because we have not taken into account a decay of the neutrino luminosity when $t \gtrsim 500$ ms (e.g., Wilson & Mayle 1988; see also Shimizu et al. 2001).

We found that there are remarkable differences in the explosion energy depending on the mode of the fluctuations and that larger number of modes in the fluctuations makes the result closer to that of spherical explosion, irrespective of the model series A or B. Any small-scale fluctuations on the neutrinosphere are greatly averaged out when the neutrino emission is observed far enough from the neutrino-emitting surface. Moreover, we found that a certain broad space is needed to be heated by neutrinos to revive the stalled shock wave rigorously and that the global anisotropy ($n_\theta = 1$) is the most effective to increase the explosion energy. Burrows et al. (1995) suggested that the neutrino flux can fluctuate not

only with angle but with time. Such time fluctuations are expected to reduce further the efficiency of anisotropy, which needs to be confirmed in the future.

4. CONCLUSION

We have investigated the effects of small-scale fluctuations in the neutrino flux on the core-collapse supernova explosion. In order to examine the effect of the degree of anisotropy itself on the explosion, we have studied two model series parametrically. We specified the neutrino radiation field taking its geometric effects into account in each model. We found that the global anisotropy ($n_\theta = 1$) and the local fluctuations ($n_\theta > 1$) in the neutrino flux have quite different effects on the explosion mechanism, that is, the shock dynamics, the explosion energy, and the explosion asymmetry. Since the small-scale fluctuations are averaged out for radiative and hydrodynamic reasons, the results including fluctuations become closer to that of spherical explosion. Consequently, the global anisotropy is the most effective mechanism of increasing the explosion energy. Note here that the explosion energy could differ substantially depending on the neutrino temperature (the difference between 4.70 and 4.65 MeV is only 1%). This indicates that the supernova problem is very sensitive to the neutrino energy and luminosity. However, the total luminosity cannot be simply increased to explain the observed explosion energy because such treatment leads to the problem of Ni overproduction, especially in the case of essentially spherical models. We therefore conclude that globally anisotropic neutrino radiation is of great importance in actual supernova explosions. This supports the claim made by Shimizu et al. (2001).

The global anisotropy can originate from rotation of a proto–neutron star or a hot spot on the neutrino-emitting region, while the small-scale fluctuations are considered to be resulted from gravitational oscillation or uniform convection. It will be very interesting if any evidence of anisotropic neutrino radiation is observed at facilities like Super Kamiokande (Hirata et al. 1987; Suzuki 1998) and SNO (Poon et al. 2001), together with detailed optical observations (e.g., Wang et al. 2002).

We are grateful to the anonymous referee for useful comments and suggestions that improved this paper.

REFERENCES

- Bruenn, S. W., Mezzacappa, A., & Dineva, T. 1995, *Phys. Rep.*, 256, 69
- Burrows, A., Hayes, J., & Fryxell, B. A. 1995, *ApJ*, 450, 830
- Colgate, S. A., & White, R. H. 1966, *ApJ*, 143, 626
- Fukuda, I. 1982, *PASP*, 94, 271
- Fryer, C. L., & Heger, A. 2000, *ApJ*, 541, 1033
- Fryer, C. L., & Warren, M. S. 2002, *ApJ*, 574, L65
- Herant, M., Benz, W., Hix, W. R., Fryer, C. L., & Colgate, S. A. 1994, *ApJ*, 435, 339
- Hirata, K. et al. 1987, *Phys. Rev. Lett.*, 58, 1490
- Janka, H.-T., & Mönchmeyer, R. 1989, *A&A*, 209, L5
- Janka, H.-T., & Müller, E. 1996, *A&A*, 306, 167
- Keil, W., Janka, H.-T., & Müller, E. 1996, *ApJ*, 473, L111
- Kifonidis, K., Plewa, T., Janka, H.-Th., & Müller, E. 2003, *A&A*, submitted (astro-ph/0302239)
- Liebendoerfer, M., Mezzacappa, A., Thielemann, F.-K, Messer, O. E. B., Hix, W. R., & Bruenn, S. W. 2001, *Phys. Rev. D*, 63, 103004
- Mezzacappa, A., Calder, A. C., Bruenn, S. W., Blondin, J. M., Guidry, M. W., Strayer, M. R., & Umar, A. S. 1998, *ApJ*, 495, 911
- Miller, D. S. , Wilson, J. R., & Mayle, R. W. 1993, *ApJ*, 415, 278
- Poon, A. W. P., et al. 2001, in *AIP Conf. Proc.* 610, *Nucl. Phys. in the 21st Century*, ed. E. Norman, L. Schroeder, & G. Wozniak (New York: AIP), 218
- Shimizu, T. M. 1995, Ph.D.thesis, Univ. Tokyo
- Shimizu, T. M., Ebisuzaki, T., Sato, K., & Yamada, S. 2001, *ApJ*, 552, 756
- Shimizu, T., Yamada, S., & Sato, K. 1994, *ApJ*, 432, L119
- Suzuki, Y. 1998, *Prog. Part. Nucl. Phys.*, 40, 427

Tassoul, J. -L. 1978, *Theory of Rotating Stars* (Princeton: Princeton Univ. Press)

Wang, L., et al. 2002, *ApJ*, 579, 671

Wilson, J. R. 1985, in *Numerical Astrophysics*, ed. J.M.Centrella, J.M.LeBlanc, & R.L.Bowers (Boston: Jones & Bartlett), 422

Wilson, J. R. & Mayle R. W. 1988, *Phys. Rep.*, 163, 63

Wilson, J. R. & Mayle R. W. 1993, *Phys. Rep.*, 227, 97

Table 1. Simulated Models

Model Series	a^a	Model	n_θ^b	c_2^c	$T_\nu^c(\text{MeV})$
A	0.31	A1-T465	1	0.100	4.65
		A1-T470	1	0.100	4.70
		A3-T465	3	0.051	4.65
		A3-T470	3	0.051	4.70
		A5-T465	5	0.035	4.65
		A5-T470	5	0.035	4.70
B	0.71	B1-T465	1	0.200	4.65
		B1-T470	1	0.200	4.70
		B3-T465	3	0.101	4.65
		B3-T470	3	0.101	4.70
		B5-T465	5	0.068	4.65
		B5-T470	5	0.068	4.70

^aMagnitude of fluctuations on the neutrino emitting surface.

^bMode number of fluctuations.

^cMagnitude of fluctuations far enough from the neutrino emitting surface.

^dTemperature on the neutrinosphere

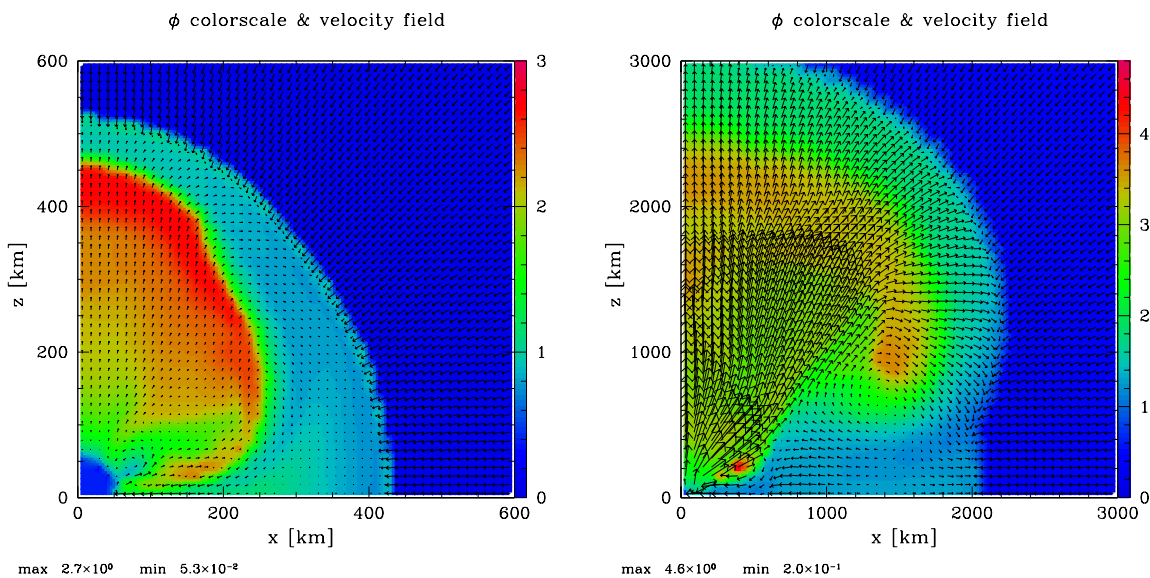


Fig. 1.— Color-scale maps of the dimensionless entropy distribution and the velocity fields for the model of $n_\theta = 1$ and $T_\nu = 4.70$ MeV of series A (model A1-T470). Left: $t = 82$ ms after the shock stall, Right: $t = 244$ ms.

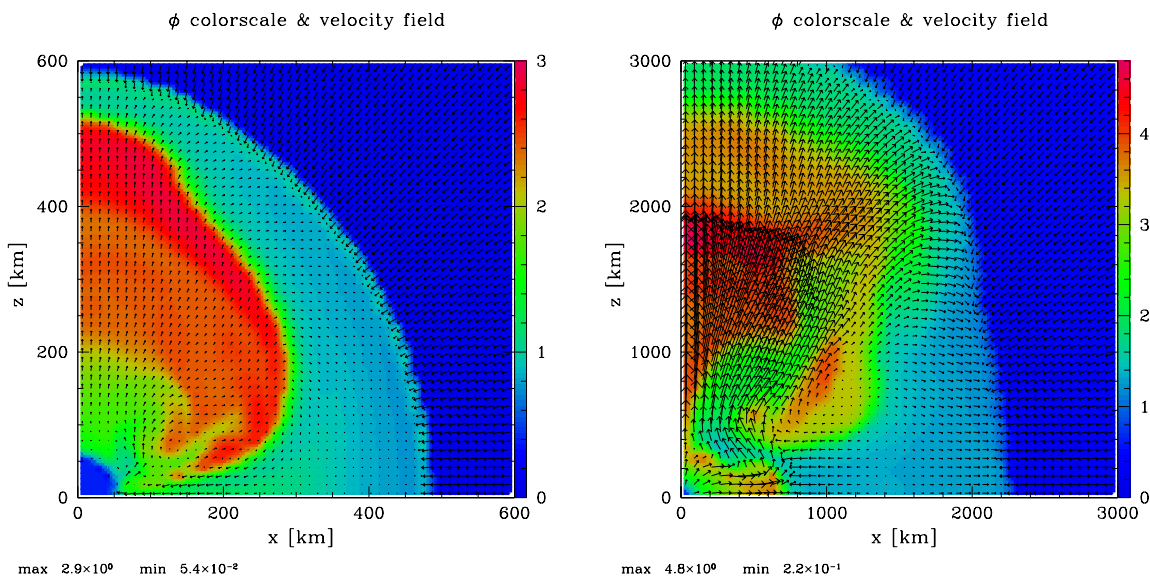


Fig. 2.— Same as Fig.1, except for series B (model B1-T470). Left: $t = 82$ ms after the shock stall, Right: $t = 249$ ms.

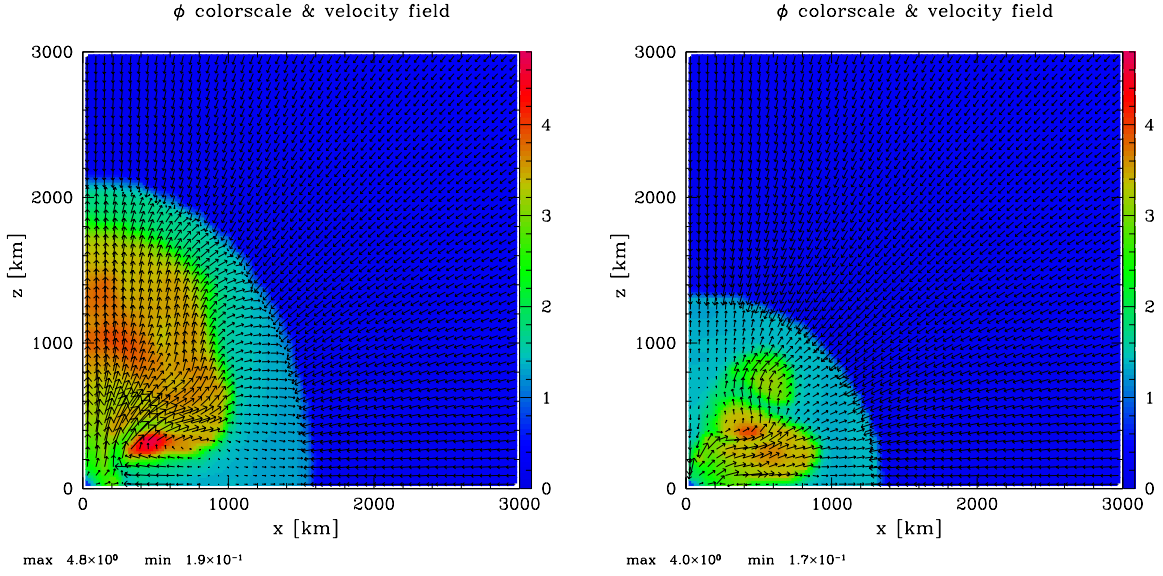


Fig. 3.— Same as Fig.1, except for the case of fluctuated neutrino flux. Left: $n_\theta = 3$ (model A3-T470) at $t = 254$ ms after the shock stall, Right: $n_\theta = 5$ (model A5-T470) at $t = 250$ ms.

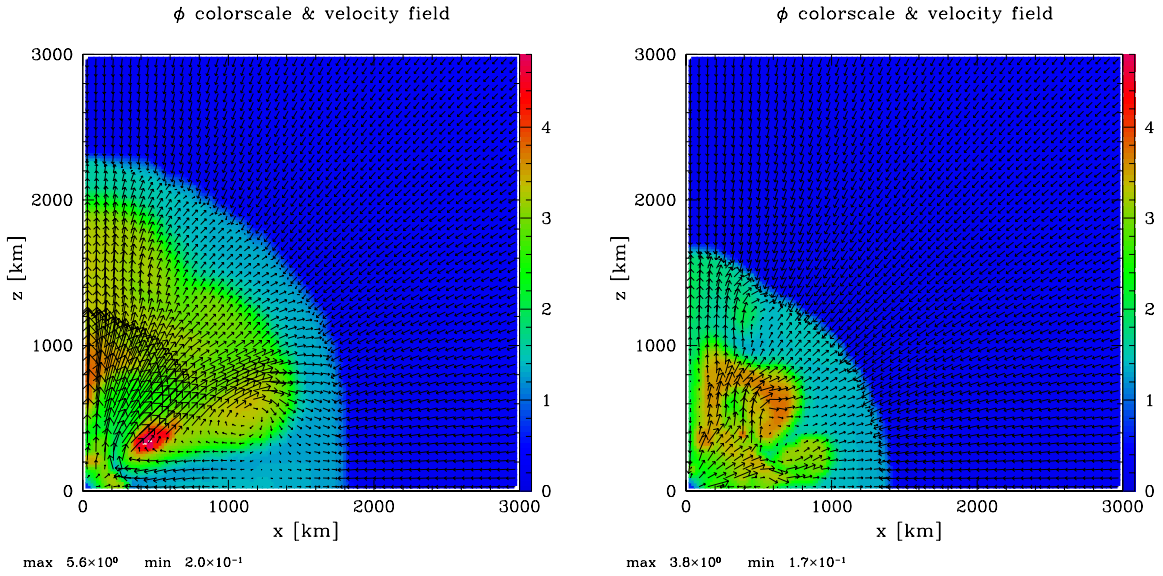


Fig. 4.— Same as Fig.3, except for series B. Left: $n_\theta = 3$ (model B3-T470) at $t = 257$ ms after the shock stall, Right: $n_\theta = 5$ (model B5-T470) at $t = 247$ ms.

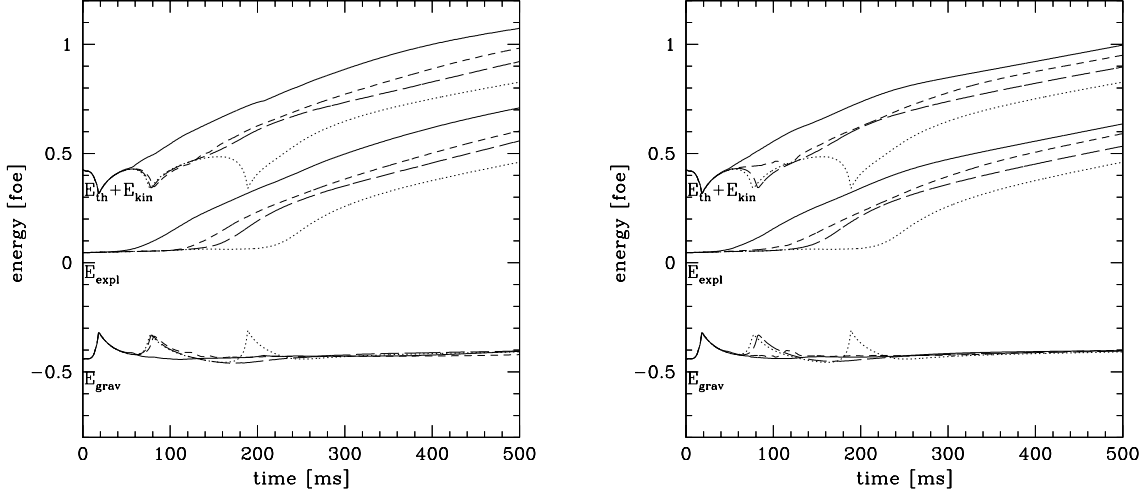


Fig. 5.— Evolution of thermal and kinetic energy ($E_{\text{th}} + E_{\text{kin}}$), gravitational energy (E_{grav}) and explosion energy (E_{expl}) for the models of $T_\nu = 4.70$ MeV. Solid line corresponds to the case of $n_\theta = 1$, short-dashed line $n_\theta = 3$, long-dashed line $n_\theta = 5$, and dotted line $c_2 = 0$ (spherical). Left: model series A, Right: model series B.

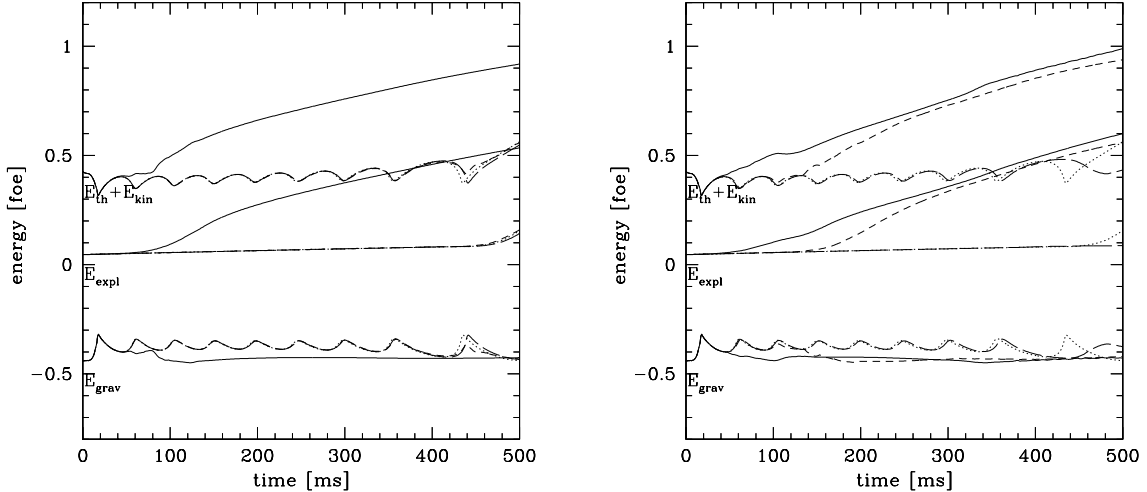


Fig. 6.— Same as Fig.5, except for $T_\nu = 4.65$ MeV. Left: model series A, Right: model series B.